

8-29-2022

A New Technique for Solving Neutral Delay Differential Equations Based on Euler Wavelets

Mutaz Mohammad
Kuban State Agrarian University

Alexander Trounev
Zayed University

Follow this and additional works at: <https://zuscholars.zu.ac.ae/works>



Part of the [Mathematics Commons](#)

Recommended Citation

Mohammad, Mutaz and Trounev, Alexander, "A New Technique for Solving Neutral Delay Differential Equations Based on Euler Wavelets" (2022). *All Works*. 5336.
<https://zuscholars.zu.ac.ae/works/5336>

This Article is brought to you for free and open access by ZU Scholars. It has been accepted for inclusion in All Works by an authorized administrator of ZU Scholars. For more information, please contact scholars@zu.ac.ae.

Research Article

A New Technique for Solving Neutral Delay Differential Equations Based on Euler Wavelets

Mutaz Mohammad ¹ and Alexander Trounev²

¹Kuban State Agrarian University, Krasnodar, Russia

²Zayed University, Abu Dhabi, UAE

Correspondence should be addressed to Mutaz Mohammad; mutaz.mohammad@zu.ac.ae

Received 27 May 2022; Accepted 24 July 2022; Published 29 August 2022

Academic Editor: Fathalla A. Rihan

Copyright © 2022 Mutaz Mohammad and Alexander Trounev. This is an open access article distributed under the Creative Commons Attribution License, which permits unrestricted use, distribution, and reproduction in any medium, provided the original work is properly cited.

An effective numerical scheme based on Euler wavelets is proposed for numerically solving a class of neutral delay differential equations. The technique explores the numerical solution via Euler wavelet truncated series generated by a set of functions and matrix inversion of some collocation points. Based on the operational matrix, the neutral delay differential equations are reduced to a system of algebraic equations, which is solved through a numerical algorithm. The effectiveness and efficiency of the technique have been illustrated by several examples of neutral delay differential equations. The main advantages and key role of using the Euler wavelets in this work lie in the performance, accuracy, and computational cost of the proposed technique.

1. Introduction

We consider the following neutral delay differential equation (NDDE) given by.

$$\begin{aligned} u'(t) &= gt, u(t), u(t - \theta(t, u(t))), \\ u'(t - \eta(t, u(t))), \quad t_1 \leq t \leq t_g, \end{aligned} \quad (1)$$

$$u(t) = \phi(t), \quad t \leq t_1, \quad (\phi \text{ is the initial function}). \quad (2)$$

such that

$$g: [t_1, t_g] \times R \times R \times R \otimes R, \quad (3)$$

is a differentiable function, θ and η are continuous functions defined on $[t_1, t_g] \times \mathbb{R}$, provided that.

$$t - \theta(t, u(t)) < t_g, \quad t - \eta(t, u(t)) < t_g. \quad (4)$$

Recently, delay differential equations (DDEs) and NDDE have been given much interest in engineering and science including physics, chemistry, and biology, for e.g., one of the rich sources of such applications can be found in [1–3]. More interesting examples and rigorous treatment are presented

in [4–7]. In [8–13], the authors developed various issues of numerical modeling involving DDEs.

The proposed problem 1 and (2) is a special class of DDE, which appears in a wide range of applications such as the mathematical modeling of ecology, electronics, and control of ships and aircraft. It is obvious that these kinds of NDDE cannot be solved exactly. Hence, it is crucial to develop efficient numerical techniques to simulate solutions of such equations. Many researchers reported several techniques in this development, for example, Runge–Kutta method has been used in [14], variational iteration method in [15], and other numerical schemes and properties can be found in [7, 16, 17].

2. The Numerical Approach Based on Euler Wavelet

Wavelet expansions and its generalization, such as framelets, have been successful in numerical simulation in many areas of applications in real-world phenomena [18]. This is largely due to the fact that wavelets have the right structure to capture the sparsity in linear systems. Note that the great

hopes in developing wavelet-based representations and theory of turbulent flows have not been materialized. Euler wavelet approximation would have the right approximating structure to be efficient for a general NDDE due to the orthogonality of the envisaged wavelets in the proposed framework. To solve the proposed problem, we use Euler wavelets generated via Euler polynomials and presented in [19].

The Euler polynomial $U_k(x)$ is defined based on the generating function that has the form.

$$\sum_{k=0}^{\infty} \frac{U_k(x)t^k}{k!} = \frac{e^{xt}}{e^t + 1}. \quad (5)$$

The first few Euler polynomials are given below, and the graphical presentation of some of these functions is presented in Figure 1.

$$U_0(x) = 1,$$

$$U_1(x) = x - \frac{1}{2},$$

$$U_2(x) = x^2 - x,$$

$$U_3(x) = x^3 - \frac{3x^2}{2} + \frac{1}{4},$$

$$U_4(x) = x^4 - 2x^3 + x, \quad (6)$$

$$U_5(x) = x^5 - \frac{5x^4}{2} + \frac{5x^2}{2} - \frac{1}{2},$$

$$U_6(x) = x^6 - 3x^5 + 5x^3 - 3x,$$

$$U_7(x) = x^7 - \frac{7x^6}{2} + \frac{35x^4}{4} - \frac{21x^2}{2} + \frac{17}{8}.$$

Let us define the Euler polynomials $U_1(x), U_2(x)$ and the needed functions in the following numerical scheme:

$$U_1(t) = -\frac{1}{2} + t, U_2(x) = -x + x^2, \quad (7)$$

$$I_1^1 = \int_0^x U_1(t)dt, \quad (8)$$

$$I_2^1 = \int_0^x U_2(t)dt, \quad (9)$$

$$I_1^2 = \int_0^x I_1^1(t)dt, \quad (10)$$

$$I_2^2 = \int_0^x I_2^1(t)dt. \quad (11)$$

Let Ξ be the set of all functions given in equations (3)–(8). For any function $\tau \in \Xi$, we define the function $\varphi(x)$ as follows:

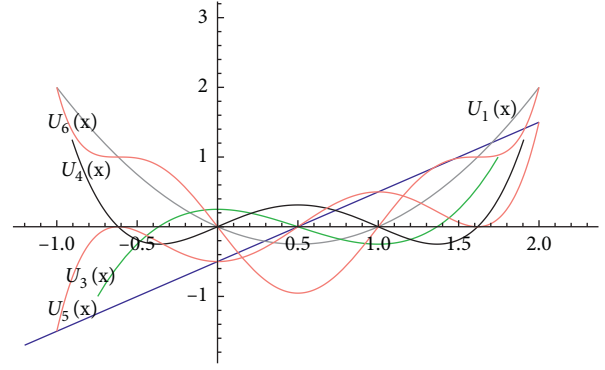


FIGURE 1: The graphs of the first few Euler polynomials U_1 through U_5 .

$$\varphi(t) = \tau \chi_{[0,1]}(t), \quad (12)$$

where $\chi_{[0,1]}$ is the indicator function on $[0,1]$. Assume that,

$$\begin{aligned} \varphi_1 &= U_1, \\ \varphi_2 &= U_2, \\ \varphi_{1,1} &= I_1^1, \\ \varphi_{2,1} &= I_2^1, \\ \varphi_{1,2} &= I_1^2, \\ \varphi_{2,2} &= I_2^2. \end{aligned} \quad (13)$$

We define the following set of wavelets, where $j, k \in \mathbb{Z}$ as,

$$\begin{aligned} \varphi_1(j, k, t) &= \varphi_1(2^j t - k), \\ \varphi_2(j, k, t) &= \varphi_2(2^j t - k), \\ \varphi(j, k, t) &= (\varphi_1(j, k, t) + \varphi_2(j, k, t)), \\ \varphi^{1,1}(j, k, t) &= \varphi_{1,1}(2^j t - k), \\ \varphi^{1,2}(j, k, t) &= \varphi_{1,2}(2^j t - k), \\ \varphi^{2,1}(j, k, t) &= \varphi_{2,1}(2^j t - k), \\ \varphi^{2,2}(j, k, t) &= \varphi_{2,2}(2^j t - k), \\ \varphi^1(j, k, t) &= \frac{(\varphi^{1,1}(j, k, t) + \varphi^{2,1}(j, k, t))}{j}, \\ \varphi^2(j, k, t) &= \frac{(\varphi^{2,1}(j, k, t) + \varphi^{2,2}(j, k, t))}{j^2}. \end{aligned} \quad (14)$$

Recall that, see for example., [20], a function $\tau \in L_2(\mathbb{R})$ can be expanded using the following series,

$$\tau(x) = \sum_{\ell=1}^2 \sum_{j,k \in \mathbb{Z}} d^\ell(j, k) \varphi^\ell(j, k, x), \quad (15)$$

where,

$$d^\ell(j, k) = \langle \tau, \varphi^\ell(j, k, x) \rangle = \int_{\mathbb{R}} \tau(x) \varphi^\ell(j, k, x) w(x) dx, \quad (16)$$

In which $\langle \cdot, \cdot \rangle$ denotes the usual inner product over the space $L_2(\mathbb{R})$ and w is a proper weight function.

One may truncate (16) by $\tau_{n,M}$ where,

$$\tau_{n,M}(t) = \sum_{\ell=1}^2 \sum_{j=0}^n \sum_{k=0}^{M-1} d^\ell(j, k) \varphi^\ell(j, k, t). \quad (17)$$

Therefore,

$$\|\tau - \tau_{n,M}\|_2^2 = \left\| \sum_{\ell=1}^2 \sum_{j \geq n+1} \sum_{k \geq M+1} d^\ell(j, k) \varphi^\ell(j, k, t) \right\|_2^2. \quad (18)$$

Notice that,

$$|\langle d^\ell(j, k) \rangle| \leq \max_t |\tau| \|\varphi^\ell(j, k, t)\|_1. \quad (19)$$

Hence based on Bessel inequality,

$$\|f - f_{n,M}\|_2^2 \leq \max_t |\tau| \|\varphi^\ell(j, k, t)\|_1 \sum_{\ell=1}^2 \sum_{j \geq n+1} \sum_{k=M}^{\infty} |d^\ell(j, k)|. \quad (20)$$

To solve the proposed problem, similar to the method in [19], we construct a vector Ξ_τ of length $M = 2^{n+1}$, $n \in \mathbb{N}$, such that

$$\Xi_\tau = [\varphi_\tau, \sigma^\kappa(1, 0, x), \dots, \sigma^\kappa(2^j, k, x), \dots, \sigma^\kappa(2^n, 2^{n-1}, x), \\ j = 0, 1, 2, \dots, n; k = 0, 1, 2, \dots, 2^{j-1}, \quad (21)$$

where,

$$\begin{cases} \varphi_\tau = 1, \sigma^\kappa = \varphi & \text{when } \tau = U_1, U_2, \kappa = 1, \\ \varphi_\tau = x, \sigma^\kappa = \varphi^1 & \text{when } \tau = I_1^1, I_2^1, \kappa = j, \\ \varphi_\tau = \frac{x^2}{2}, \sigma^\kappa = \varphi^2 & \text{when } \tau = I_1^2, I_2^2, \kappa = j^2. \end{cases} \quad (22)$$

As an illustration, when $n = 2$, we have the following equations:

(i) When $\varphi_\tau = 1, \kappa = 1$, we have the following equation:

$$\Xi_\tau = \begin{cases} [1, 0, \dots, 0] & x \in \mathbb{R} - [0, 1) \\ [1, x^2 - 0.5, 0, 4x^2 - 4x + 0.5, 0, 0, 0, 16x^2 - 24x + 8.5] & x \in [0.75, 1) \\ [1, x^2 - 0.5, 0, x^2 - 4x + 0.5, 0, 0, 16x^2 - 16x + 3.5, 0] & x \in [0.5, 0.75) \\ [1, x^2 - 0.5, 4x^2 - 0.5, 0, 0, 0.5 - 8x + 16x^2, 0, 0] & x \in [0.25, 0.5) \\ [1, x^2 - 0.5, 4x^2 - 0.5, 0, 16x^2 - 0.5, 0, 0, 0] & \text{True} \end{cases} \quad (23)$$

(ii) When $\varphi_\tau = x, \kappa = j$, we have the following equation:

$$\Xi_\tau = \begin{cases} [x, 0, \dots, 0] & x \in \mathbb{R} - [0, 1) \\ \left[x, \frac{x^3}{3} - \frac{x}{2}, 0, \frac{4x^3}{3} - 2x^2 + \frac{x}{2} + \frac{1}{12}, 0, 0, 0, \frac{16x^3}{3} - 12x^2 + \frac{17x}{2} - \frac{15}{8} \right] & x \in [0.75, 1) \\ \left[x, \frac{x^3}{3} - \frac{x}{2}, 0, \frac{4x^3}{3} - 2x^2 + \frac{x}{2} + 0.0833333, 0, 0, \frac{16x^3}{3} - 8x^2 + \frac{7x}{2} - \frac{5}{12}, 0 \right] & x \in [0.5, 0.75) \\ \left[x, \frac{x^3}{3} - \frac{x}{2}, \frac{4x^3}{3} - \frac{x}{2}, 0, 0, \frac{16x^3}{3} - 4x^2 + \frac{x}{2} + \frac{1}{24}, 0, 0 \right] & x \in [0.25, 0.5) \\ \left[x, \frac{x^3}{3} - \frac{x}{2}, \frac{4x^3}{3} - \frac{x}{2}, 0, \frac{16x^3}{3} - \frac{x}{2}, 0, 0, 0 \right] & \text{True} \end{cases} \quad (24)$$

(iii) When $\varphi_\tau = x^2/2, \kappa = j^2$, we have the following equation:

$$\Xi_\tau = \begin{cases} [0.5x^2, 0, \dots, 0] & x \in \mathbb{R} - [0, 1) \\ \left[0.5x^2, \frac{x^4}{12} - \frac{x^2}{4}, 0, \frac{x^4}{3} - \frac{2x^3}{3} + \frac{x^2}{4} + \frac{x}{12} - \frac{1}{24}, 0, 0, 0, \frac{4x^4}{3} - 4x^3 + \frac{17x^2}{4} - \frac{15x}{8} + \frac{9}{32} \right] & x \in [0.75, 1) \\ \left[0.5x^2, \frac{x^4}{12} - \frac{x^2}{4}, 0, \frac{x^4}{3} - \frac{2x^3}{3} + \frac{x^2}{4} + \frac{x}{12} - \frac{1}{24}, 0, 0, \frac{4x^4}{3} - \frac{8x^3}{3} + \frac{7x^2}{4} - \frac{5x}{12} + \frac{1}{48}, 0 \right] & x \in [0.5, 0.75) \\ \left[0.5x^2, \frac{x^4}{12} - \frac{x^2}{4}, \frac{x^4}{3} - \frac{x^2}{4}, 0, 0, 48x^4 - 28x^3 - \frac{47x^2}{12} + \frac{11x}{24} - \frac{1}{96}, 0, 0 \right] & x \in [0.25, 0.5) \\ \left[0.5x^2, \frac{x^4}{12} - \frac{x^2}{4}, \frac{x^4}{3} - \frac{x^2}{4}, 0, \frac{4x^4}{3} - \frac{x^2}{4}, 0, 0, 0 \right] & \text{True} \end{cases} \quad (25)$$

Now, let us define the solution of equations (1) and (2) via the form of matrices based on the above approach. Assume the Euler wavelet truncated expansion given by equation (10) to be defined as follows:

$$u'(t) = \sum_{\ell=1}^2 \sum_{j=0}^n \sum_{k=0}^{M-1} d^\ell(j, k) \varphi^\ell(j, k, t). \quad (26)$$

Then,

$$u(t) = u(0) + \sum_{\ell=1}^2 \sum_{j=0}^n \sum_{k=0}^{M-1} \int_0^t d^\ell(j, k) \varphi^\ell(j, k, x) dx. \quad (27)$$

Additionally,

$$u'(t - \eta(t, u(t))) = \sum_{\ell=1}^2 \sum_{j=0}^n \sum_{k=0}^{M-1} d^\ell(j, k) \varphi^\ell(j, k, t - \eta(t, u(t))). \quad (28)$$

Note that from (28), we have the following equation:

$$u(t - \theta(t, u(t))) = u(0) + \sum_{\ell=1}^2 \sum_{j=0}^n \sum_{k=0}^{M-1} \int_0^t d^\ell(j, k) \varphi^\ell(j, k, x - \theta(x, u(x))) dx. \quad (29)$$

Assume that $I_{j,k}^\ell(t) = \int_0^t \varphi^\ell(j, k, x) dx$. Substituting equations (11)–(14) in equations (1) and (2) yields,

$$\begin{aligned} & \sum_{\ell=1}^2 \sum_{j=0}^n \sum_{k=0}^{M-1} d^\ell(j, k) \varphi^\ell(j, k, t - \eta(t, u(t))) \\ &= g \left(t, u(0) + \sum_{\ell=1}^2 \sum_{j=0}^n \sum_{k=0}^{M-1} d^\ell(j, k) I_{j,k}^\ell(t), u(0) + \sum_{\ell=1}^2 \sum_{j=0}^n \sum_{k=0}^{M-1} d^\ell(j, k) I_{j,k}^\ell(t) \right) \\ & \sum_{\ell=1}^2 \sum_{j=0}^n \sum_{k=0}^{M-1} d^\ell(j, k) \varphi^\ell(j, k, t - \eta(t, u(t))) \end{aligned} \quad (30)$$

The needed functions for the numerical scheme are ready to be used and so we define,

$$M = 2^{1+n}, n = 1, 2, \dots, \quad (31)$$

As a collocation node where

$$\begin{aligned} s_i &= \frac{s_{i-1} + 1}{M}, i = 1, 2, \dots, M; t_i \\ &= \frac{1}{2} (s_{i-1} + s_i), i = 1, 2, \dots, M. \end{aligned} \quad (32)$$

Hence, by substituting the proposed collocation points to the equation above, we get the following equation:

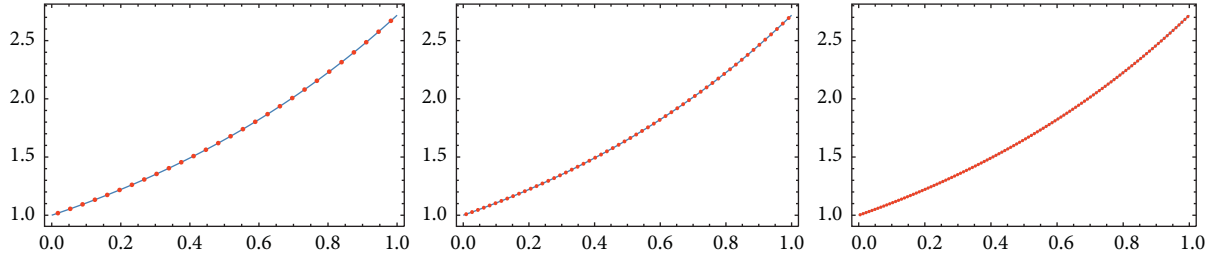


FIGURE 2: Illustration of example 1 for the analytical and numerical solution (dots) computed with 28, 56, and 112 collocation points.

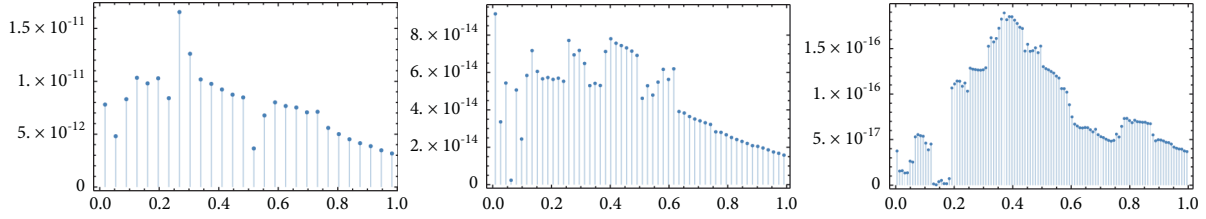


FIGURE 3: Absolute maximum errors in example 1 when $M = 3, 4, 5$, respectively.

$$\begin{aligned}
 & u(0) + \sum_{\ell=1}^2 \sum_{j=0}^n \sum_{k=0}^{M-1} d^{\ell}(j, k) I_{j, k}^{\ell}(t_i), \\
 & g\left(t_i, u(0) + \sum_{\ell=1}^2 \sum_{j=0}^n \sum_{k=0}^{M-1} d^{\ell}(j, k) I_{j, k}^{\ell}(t_i),\right. \\
 & \left. u(0) + \sum_{\ell=1}^2 \sum_{j=0}^n \sum_{k=0}^{M-1} d^{\ell}(j, k) I_{j, k}^{\ell}(t_i),\right. \\
 & \left. \sum_{\ell=1}^2 \sum_{j=0}^n \sum_{k=0}^{M-1} d^{\ell}(j, k) \varphi^{\ell}(j, k, t_i - \eta(t, u(t_i)))\right).
 \end{aligned} \tag{33}$$

Note that implementing the collocation division generates a system of algebraic equations that can be solved easily, for example using Mathematica software 13.0 to produce the unknown coefficients $d^{\ell}(j, k)$ needed to find an approximate solution given by (28).

3. Numerical Illustration

In this part, we illustrate some examples of the proposed NDDE problem based on the presented numerical scheme and obtain some maximum absolute errors. The numerical evidences showed high accuracy compared with the exact ones. Six examples will be illustrated. For examples 1–3 from [21], we got an absolute error decreasing from 10^{-12} by 28 collocation points to 10^{-18} by 112 collocation points. In example 4, we got zero absolute error. Throughout the presented figures and numerical results, the algorithm demonstrates the accuracy and excellent agreement between the numerical solutions and the exact ones.

TABLE 1: Some numerical evidences for the errors in example 1, with 28 collocation points.

x	Error bound
0.0178571	7.79821×10^{-12}
0.0535714	4.80194×10^{-12}
0.0892857	8.30580×10^{-12}
0.1250000	1.03304×10^{-11}
0.1607140	9.80105×10^{-12}
0.8035710	5.00178×10^{-12}
0.8392860	4.51461×10^{-12}
0.8750000	4.14158×10^{-12}
0.9107140	3.86313×10^{-12}
0.9464290	3.46967×10^{-12}
0.9821430	3.16769×10^{-12}

Example 1. Let's take the following NDDE

$$\frac{du}{dt} + (\cos(t))^{1/2} (u'(t^{1/2}) - e^{t^{1/2}}) \tag{34}$$

$$+ (\sin(t^{1/2}) + e^t) (u(\sin(t)) - e^{\sin(t)}) = e^t, 0 \leq t \leq 1.$$

The initial condition for this formulation is given by,

$$u(t) = e^t, t \leq 0. \tag{35}$$

The exact solution is defined as follows:

$$u(t) = e^t. \tag{36}$$

The exact and approximate solutions for different number of collocation points are presented in Figures 2 and 3, where the agreement between the approximate and exact functions and the error bounds are clearly improved gradually when the order of the partial sum of the truncated Euler series expansion enlarges. In Table 1, we show the error bound resulted for example 1.

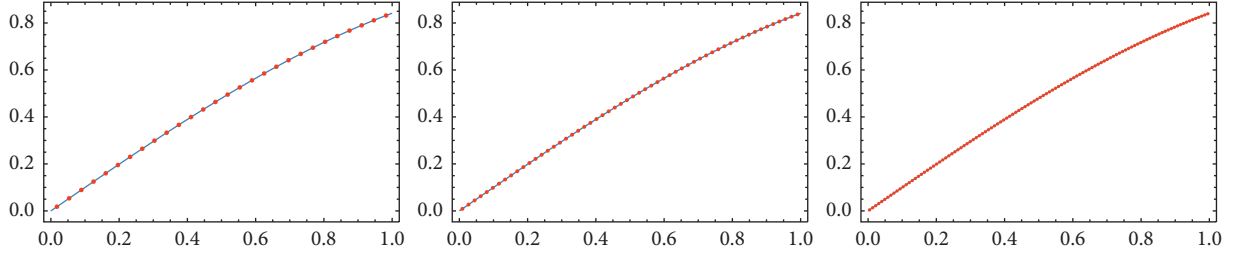


FIGURE 4: Illustration of Example 2 for the analytical and numerical solution (dots) computed with 28, 56, and 112 collocation points.

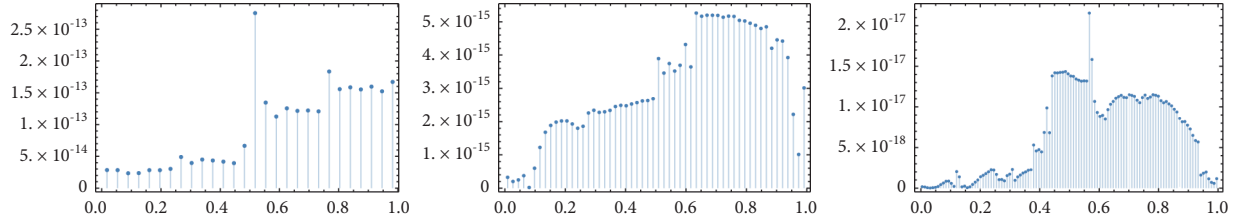


FIGURE 5: Absolute maximum errors in Example 2 when $M = 3, 4, 5$, respectively.

Example 2. Here we take the NDDE

$$\begin{aligned} \frac{du}{dt} + t^{1/2}(u'(e^{-t/2}) - u(t^{1/2}e^{-t}) + u(t) - \cos(e^{-t/2})) \\ - \sin(t^{1/2}e^{-t}) + \sin(t) = \cos(t), 0 \leq t \leq 1, \end{aligned} \quad (37)$$

where the initial condition is as follows:

$$u(t) = \sin(t), \quad t \leq 0. \quad (38)$$

The exact solution is as follows:

$$u(t) = \sin(t). \quad (39)$$

Similarly, both the exact and approximate solutions for different number of collocation points are depicted in Figures 4 and 5 and we illustrate the error bound for example 1 in Table 2, where again the improvement of the numerical approximation is clearly shown in the graphical and numerical evidences.

Example 3. Consider the following NDDE

$$\begin{aligned} \frac{du}{dt} - \frac{1}{2}u'\left(\frac{4}{5}t\right) - \frac{1}{10}u\left(\frac{4}{5}t\right) - u(t) \\ + \left(\frac{4}{5}t - \frac{1}{2}\right)e^{\frac{4}{5}t} = e^{-t}, 0 \leq t \leq 1, \end{aligned} \quad (40)$$

where the initial condition for this formulation is given by,

$$u(0) = 0, \quad t \leq 0. \quad (41)$$

The exact solution is given by,

$$u(t) = te^{-t}. \quad (42)$$

Another graphical and numerical evidences are presented in Figures 6, 7, and Table 3.

TABLE 2: Some numerical evidences for the errors in example 2, with 28 collocation points.

x	Error bound
0.0178571	2.84662×10^{-14}
0.0535714	2.83601×10^{-14}
0.0892857	2.34596×10^{-14}
0.1250000	2.36812×10^{-14}
0.1607140	2.83169×10^{-14}
0.8035710	1.55746×10^{-13}
0.8392860	1.58554×10^{-13}
0.8750000	1.55258×10^{-13}
0.9107140	1.59703×10^{-13}
0.9464290	1.52353×10^{-13}
0.9821430	1.67129×10^{-12}

Example 4. Consider the following NDDE arising in electrodynamics

$$\begin{aligned} \frac{du}{dt} - 3\left(t^2 + \frac{t}{6} + 2\right)u\left(\frac{t}{6}\right) = \left(-\frac{t^4}{12} + \frac{193t^3}{360} + \frac{3749t^2}{588} + \frac{30t}{7} - 1\right) \\ - u'(t) - 4(t+2)u\left(\frac{t}{4}\right) \\ + 5tu\left(\frac{t}{5}\right) + 2u\left(\frac{t}{7}\right), 0 \leq t \leq 1, \end{aligned} \quad (43)$$

where the initial condition for this formulation is given by,

$$u(0) = 2, \quad t \leq 0. \quad (44)$$

The exact solution is given by

$$u(t) = 2 + t - t^2. \quad (45)$$

The approximate solution u_e for 7 collocation points is given by

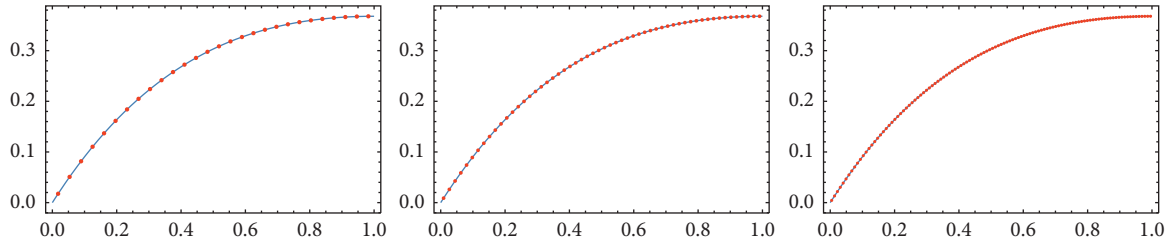


FIGURE 6: Illustration of Example 3 for the analytical and numerical solution (dots) computed with 28, 56, and 112 collocation points.

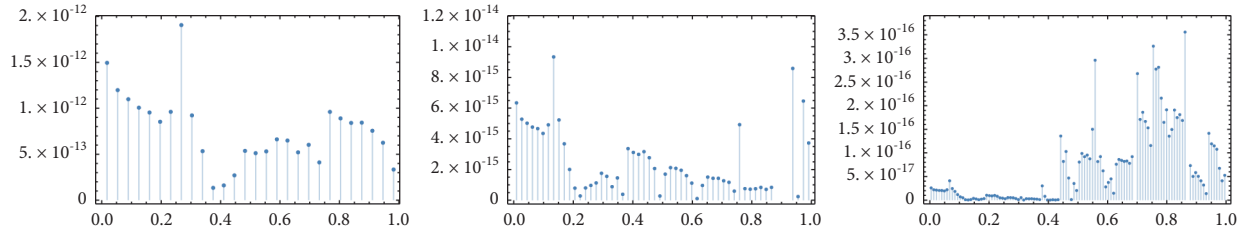


FIGURE 7: Absolute maximum errors in Example 3 when $M = 3, 4, 5$, respectively.

TABLE 3: Some numerical evidences for the errors in Example 3, with 28 collocation points.

x	Error bound
0.0178571	1.49479×10^{-12}
0.0535714	1.19775×10^{-12}
0.0892857	1.09876×10^{-12}
0.1250000	1.00640×10^{-12}
0.1607140	9.53904×10^{-13}
0.8035710	8.90010×10^{-13}
0.8392860	8.40772×10^{-13}
0.8750000	8.43603×10^{-13}
0.9107140	7.55229×10^{-13}
0.9464290	6.25056×10^{-13}
0.9821430	3.33067×10^{-12}

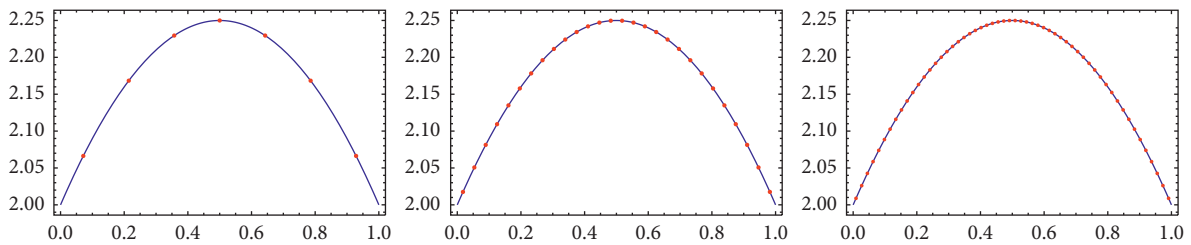


FIGURE 8: Illustration of example 4 for the analytical and numerical solution (dots) computed with 28, 56, and 112 collocation points.

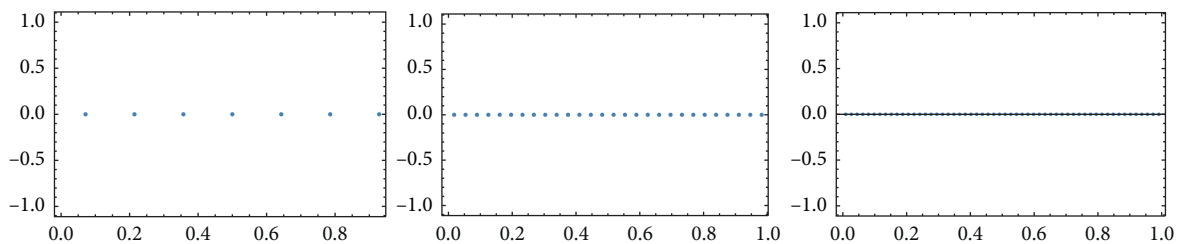


FIGURE 9: Absolute maximum errors in example 4 when $M = 1, 4, 5$, respectively.

$$\begin{aligned}
 u_e(t) = & 2 + t - t^2 - 2.14603 \times 10^{-37} t^3 + 6.49387 \\
 & \times 10^{-37} t^4 - 1.02869 \times 10^{-36} t^5 \\
 & + 8.05867 \times 10^{-37} t^6 - 2.46105 \times 10^{-37} t^7.
 \end{aligned} \quad (46)$$

Lastly, we depict the graph of the approximate and exact solutions in Figure 8, where the accuracy is presented in Figure 9.

4. Conclusion

In this presented work, a new numerical scheme based on a certain wavelet settings generated by the Euler functions is proposed. The collocation technique has been implemented on the neutral delay differential equations. We demonstrated the Euler wavelet truncated expansions to convert the resulted equations to a system of algebraic equations. We illustrated the work by solving numerically a set of problems, which arise in many scientific areas. The numerical results achieved an exceptional absolute error among other methods known in the literature. The error and approximate solutions of the given problems have been depicted by some figures to show the accuracy of the algorithm.

The main advantage of the presented algorithm is to shed some lights on the use of Euler wavelets and to develop a suitable computational technique for the numerical treatment of neural delay differential equations on a side, and on the effectiveness, efficiency of the technique in the performance, accuracy, and computational cost even with a small number of collocation points, on the other side.

Data Availability

No data were used to support this study.

Conflicts of Interest

The authors declare that they have no conflicts of interest.

Acknowledgments

This study was supported by Zayed University and UAE University Fund # 12S107UAEU-ZU-2022.

References

- [1] F. A. Rihan, *Delay Differential Equations and Applications to Biology*, Springer, Berlin, Germany, 2021.
- [2] F. A. Rihan, E. H. Doha, M. I. Hassan, and N. M. Kamel, *Numerical Treatments for Volterra Delay Integro-differential Equations*, vol. 9, no. 3, pp. 292–308, 2009.
- [3] G. A. Bocharov and F. A. Rihan, “Numerical modeling in biosciences using delay differential equations,” *Journal of Computational and Applied Mathematics*, vol. 125, no. 1-2, pp. 183–199, 2000.
- [4] Y. Kyrychko and S. Hogan, “On the use of delay equations in engineering applications,” *Journal of Vibration and Control*, vol. 16, pp. 943–960, 2010.
- [5] V. Kolmanovskii and A. Myshkis, *Introduction to the Theory and Applications of Functional Differential Equations*, Springer, Berlin, Germany, 1999.
- [6] D. Nagy, L. Bencsik, and T. Insperger, “Experimental estimation of tactile reaction delay during stick balancing using cepstral analysis,” *Mechanical Systems and Signal Processing*, vol. 138, 2020.
- [7] C. Jamilla, R. Mendoza, and V. Mendoza, “Explicit solution of a Lotka-Sharpe-McKendrick system involving neutral delay differential equations using the R-Lambert W function,” *Mathematical Biosciences and Engineering*, vol. 17, pp. 5686–5708, 2020.
- [8] B. Pao, C. Liu, and G. Yin, *Topics in Stochastic Analysis and Nonparametric Estimation*, Science Business Media, New York, 2008.
- [9] R. Driver, “Ordinary and delay differential equations,” *Applied Mathematical Sciences*, pp. 225–331, Springer-Verlag, New York-Heidelberg, 1977.
- [10] K. Gopalsamy, “Stability and oscillations in delay differential equations of population dynamics,” *Mathematics and its Applications*, vol. 74, pp. 394–461, Kluwer Academic Publishers Group, Dordrecht, 1992.
- [11] E. Lelarsmee, A. Ruehli, and S. Vincentelli, “The waveform relaxation method for time domain analysis of large scale integrated circuits,” *IEEE Trans. CAD*, vol. 1, no. 3, pp. 131–145, 1982.
- [12] J. Hale, *Theory of Functional Differential Equations*, Springer, NY, USA, 1977.
- [13] O. Bazighifan and T. Abdeljawad, “Improved approach for studying oscillatory properties of fourth-order advanced differential equations with p-laplacian like operator,” *Mathematics*, vol. 8, no. 5, p. 821, 2020.
- [14] A. Bellen and M. Zennaro, “Adaptive integration of delay differential equations,” *Advances in time-delay systems*, Springer, Berlin, 2004.
- [15] W. Wang, Y. Zhang, and S. Li, “Stability of continuous Runge-Kutta-type methods for nonlinear neutral delay-differential equations,” *Applied Mathematical Modelling*, vol. 33, no. 8, pp. 3319–3329, 2009.
- [16] M. Maleki and A. Davari, “Analysis of an adaptive collocation solution for retarded and neutral delay systems,” *Numerical Algorithms*, vol. 88, pp. 67–91, 2021.
- [17] L. Berezansky and E. Braverman, “Asymptotic properties of neutral type linear systems,” *Journal of Mathematical Analysis and Applications*, vol. 497, 2021.
- [18] M. Mohammad and A. Trounev, “On the dynamical modeling of Covid-19 involving Atangana-Baleanu fractional derivative and based on Daubechies framelet simulations, Chaos,” *Solitons & Fractals*, vol. 140, 2020.
- [19] M. Mohammad, A. Trounev, and M. Alshbool, “A novel numerical method for solving fractional diffusion-wave and nonlinear fredholm and volterra integral equations with zero absolute error,” *Axioms*, vol. 10, no. 3, p. 165, 2021.
- [20] M. Mohammad and E. B. Lin, “Gibbs phenomenon in tight framelet expansions,” *Communications in Nonlinear Science and Numerical Simulation*, vol. 55, pp. 84–92, 2018.
- [21] A. Raza and A. Khan, “Haar wavelet series solution for solving neutral delay differential equations,” *Journal of King Saud University Science*, vol. 31, pp. 1070–1076, 2019.